

---

# Augmentation-aware Self-supervised Learning with Conditioned Projector

---

Marcin Przewięzlikowski<sup>1,2,3</sup> \* Mateusz Pyla<sup>1,2,3</sup> Bartosz Zieliński<sup>1,3</sup>

Bartłomiej Twardowski<sup>3,4,5</sup> Jacek Tabor<sup>1</sup> Marek Śmieja<sup>1</sup>

<sup>1</sup> Jagiellonian University, Faculty of Mathematics and Computer Science

<sup>2</sup> Jagiellonian University, Doctoral School of Exact and Natural Sciences

<sup>3</sup> IDEAS NCBR <sup>4</sup> Department of Computer Science, Universitat Autònoma de Barcelona

<sup>5</sup> Computer Vision Center, Barcelona

## Abstract

Self-supervised learning (SSL) is a powerful technique for learning from unlabeled data. By learning to remain invariant to applied data augmentations, methods such as SimCLR and MoCo can reach quality on par with supervised approaches. However, this invariance may be detrimental for solving downstream tasks that depend on traits affected by augmentations used during pretraining, such as color. In this paper, we propose to foster sensitivity to such characteristics in the representation space by modifying the projector network, a common component of self-supervised architectures. Specifically, we supplement the projector with information about augmentations applied to images. For the projector to take advantage of this auxiliary conditioning when solving the SSL task, the feature extractor learns to preserve the augmentation information in its representations. Our approach, coined **Conditional Augmentation-aware Self-supervised Learning (CASSLE)**, is directly applicable to typical joint-embedding SSL methods regardless of their objective functions. Moreover, it does not require major changes in the network architecture or prior knowledge of downstream tasks. In addition to an analysis of sensitivity towards different data augmentations, we conduct a series of experiments, which show that CASSLE improves over various SSL methods, reaching state-of-the-art performance in multiple downstream tasks.<sup>2</sup>

## 1 Introduction

Artificial neural networks have proven to be a successful family of models in several domains, including, but not limited to, computer vision [34], natural language processing [10], solving problems at the human level with reinforcement learning [45], and biosignal processing in medicine [40]. This success is attributed largely to their ability to learn useful feature representations [29] without additional effort for input signals preparation. However, training large deep learning models requires extensive amounts of data, which can be costly to prepare, especially when human annotation is needed [2, 36].

High-quality image representations can be acquired without relying on explicitly labeled data by utilizing Self-supervised learning (SSL). A Self-supervised model is trained once on a large dataset without labels and then transferred to different downstream tasks. Initially, self-supervised methods addressed well-defined pretext tasks, such as predicting rotation [28] or determining patch position [21]. Recent studies in SSL proposed contrastive methods of learning representations that remain invariant when subjected to various data augmentations [33, 14, 17] leading to impressive results that have greatly diminished the disparity with representations learned in a supervised way [12].

---

\*Corresponding author: marcin.przewiezlikowski@doctoral.uj.edu.pl

<sup>2</sup>A short version of this paper appeared at the NeurIPS 2023 Workshop: Self-Supervised Learning - Theory and Practice. The full paper was published (OA) in Knowledge-Based Systems.

Nevertheless, contrastive methods may perform poorly when a particular downstream task relies on features affected by augmentation [67]. For example, color jittering can result in a representation space invariant to color shifts, which would be detrimental to the task of flower classification (see Figure 1). Without prior knowledge of possible downstream tasks, this effect is hard to mitigate in contrastive learning [60, 67]. Solutions for retaining information about used data augmentations in the feature extractor representation include forcing it explicitly with a modified training scheme [67, 41, 68], or by preparing a feature extractor to be adapted to a specific downstream task, e.g., with hypernetworks [13]. However, these approaches often involve significant modifications either to the contrastive model architecture [67], training procedure [41, 68], or costly training of additional models [13].

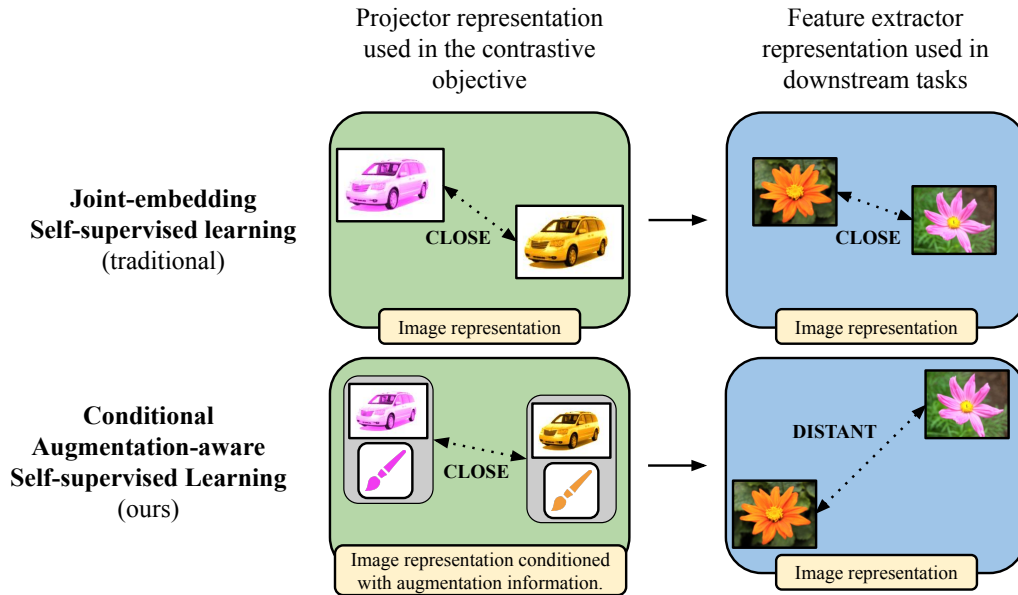


Figure 1: In the traditional self-supervised setting, contrastive loss minimization pulls the representations of augmented image views closer in the latent space of the projector (left). This may also reduce the distance between their feature extractor representations (right). Thus, the representation becomes invariant to augmentation-induced perturbations, which may hinder the performance on downstream tasks. In contrast, the self-supervised objective of CASSLE draws together joint representations of images and their augmentations in the projector space (bottom row). By conditioning the projector with augmentation information, image representations retain more sensitivity to perturbations in the feature extractor space. This proves to be beneficial when solving downstream tasks.

In this work, we propose a new method called **Conditional Augmentation-aware Self-supervised Learning (CASSLE)** that mitigates augmentation invariance of representation without neither major changes in network architecture or modifications to the self-supervised training objective. We propose to use the augmentation information during the SSL training as additional conditioning for the projector network. This encourages the feature extractor network to retain information about augmented image features in its representation. CASSLE can be applied to any joint-embedding SSL method regardless of its objective [16, 14, 17, 71, 18]. The outcome is a general-purpose, augmentation-aware encoder that can be directly used for any downstream task. CASSLE presents improved results in comparison to other augmentation-aware SSL methods, improving transferability to downstream tasks where invariance of the model representation to specific data changes could prove detrimental.

### The main contributions of our work are threefold:

- We propose a simple yet effective method for Conditional Augmentation-aware Self-supervised Learning (CASSLE). Using our conditioned projector enables preserving more information about augmentations in representations than in existing methods.
- CASSLE is a general modification that can be directly applied to existing joint-embedding SSL approaches without introducing additional objectives and major changes in the network architecture.
- In a series of experiments we demonstrate that CASSLE reaches state-of-the-art performance with different SSL methods for robust representation learning and improves upon the performance of previous augmentation-aware approaches. Furthermore, our analysis indicates that CASSLE learns representations with increased augmentation sensitivity compared to other approaches.

This manuscript is structured as follows: In Section 2, we give an overview of prior works in SSL, with a special focus on the line of work on augmentation-aware SSL. Section 3 presents our proposed technique, CASSLE. In Section 4, we conduct a thorough experimental analysis of CASSLE, in terms of its performance and unique properties. Section 5 concludes the manuscript.

## 2 Related work

In this section, we describe prior works on self-supervised learning, with a focus on computer vision. We then recall the line of work on augmentation-awareness of self-supervised models, which motivates our paper. Finally, we briefly compare our proposed method with techniques proposed in previous works.

**Self-supervised learning** (SSL) is a paradigm of learning representations from unlabeled data that can later be used for downstream tasks defined by human annotations [1, 3]. Despite learning artificial *pretext tasks*, instead of data-defined ones, SSL models have achieved tremendous success in a plethora of domains [20, 65, 58, 6]. This includes computer vision, where a variety of pretext tasks has been proposed [21, 73, 47, 28]. However, arguably the most prominent and successful SSL technique to emerge in recent years is the training of joint-embedding models for augmentation invariance [5, 62], defined by objectives such as contrastive InfoNCE (Information Noise-Contrastive Estimation) loss [33, 14, 16], self-distillation [30, 14, 48] or CCA (Canonical Correlation Analysis) [11, 71, 4]. Those objectives are often collectively referred to as *contrastive objectives* [61, 3]. A common component of joint-embedding architectures is the *projector network*, which maps representations of the feature extractor into the space where the contrastive objective is imposed [14, 16]. The usefulness of the projector has been explained through the lens of transfer learning, where it is often better to transfer intermediate network representations, to reduce the biases from the pretraining task [70, 8]. The projector also helps to mitigate the noisy data augmentations and enforces some degree of pairwise independence of image features [3, 44].

**Augmentation invariance of self-supervised models** is a natural consequence of training them with contrastive objectives, as SSL methods are prone to suppressing features that are not useful for optimizing the contrastive objectives [15, 55]. While a common set of augmentations demonstrated to typically work well on natural images in SSL has been established in the literature [33, 14, 17, 11, 74], the optimal choice of augmentations varies between specific tasks [60, 23]. [67] find that augmentation invariance can hinder the model performance on downstream tasks that require attention to precisely those traits that it had been previously trained to be invariant to. On the other hand, [72] observe that the objective of predicting augmentation parameters can in itself be a useful pretext task for SSL. Those works inspired several techniques of retaining augmentation-specific information in joint-embedding models, such as projectors sensitive to different augmentation types [67, 23], adding an objective of explicit prediction of augmentation parameters [41], , as well as task-specific pretraining [53, 63]. The above approaches produce general-purpose feature extractors that can be transferred to downstream tasks without further tuning their parameters. However, they often involve complex modifications either to the SSL model architecture [67], training procedure [41, 68], or simply tedious task-specific pretraining [63]. Another line of work proposes to train Hypernetworks [31] which produce feature extractors invariant to chosen subsets of augmentations – a more elastic, but considerably harder to train approach [13]. Several works have proposed fostering the equivariance of representations to data transformations using augmentation

information.[68] modulate the contrastive objective with augmentation strength, [7] use augmentation information as a signal for equivariance regularization in the supervised setting, whereas [27] extend the VicReg (Variance-Invariance-Covariance Regularization) [4] objective with a predictor whose parameters are generated from augmentation information by a hypernetwork [31].

**Novelty of CASSLE** We follow the line of works that aim to use augmentation information to improve the Self-supervised training of general-purpose natural image feature extractors [67, 41, 13]. Contrary to the above works, we do not make any modifications to the objective functions of the extended approaches. This removes the need to balance the invariance and sensitivity objectives, present in [41, 27]. As opposed to [67], we optimize only a single invariance objective, instead of multiple objectives dedicated to each augmentation type. Compared to [13], our method of conditioning is more straightforward to integrate into SSL training mechanisms, as we do not require all samples in a data batch to be augmented in the same way. We also do not make any modifications to the architecture of the feature extractor, unlike [13], where the feature extractor parameters are set based on augmentation parameters. In CASSLE, the feature extractor is thus much easier to use out of the box.

From a technical perspective, we compare CASSLE and other augmentation-aware SSL approaches on a wide variety of image processing tasks, including image classification, object detection, image retrieval, and rotation prediction. Moreover, we show how the InfoNCE can serve as a useful measure for comparing augmentation-awareness. To the best of our knowledge, we are the first to identify the difference between augmented and non-augmented data as a useful conditioning signal. We are also the first to analyze the masked image modeling of SSL models in terms of augmentation-awareness. Overall, our experiments provide a comparison of a variety of augmentation-aware approaches, providing guidelines for SSL practitioners.

### 3 Method

In this section, we present our approach, **Conditional Augmentation-aware Self-supervised learning (CASSLE)**. Section 3.1 provides background on joint-embedding self-supervised methods and their limitations. Section 3.2 explains the essence of CASSLE and how it leverages augmentation information to improve the quality of learned representations. Section 3.3 details the practical implementation of CASSLE’s conditioning mechanism.

Table 1: Glossary of the key concepts used in this manuscript.

	<b>Symbol</b>	<b>Explanation</b>
<b>Variables</b>	$\mathbf{x} \in \mathcal{X} \subset \mathbb{R}^D$	Data sample
	$\omega \in \Omega \subset \mathbb{R}^A$	Augmentation information vector
	$\mathbf{v} \in \mathcal{X} \subset \mathbb{R}^D$	Augmented data sample
	$\mathbf{e} \in \mathbb{R}^E$	Feature extractor embedding
<b>Functions</b>	$t_\omega : \mathcal{X} \rightarrow \mathcal{X}$	Augmentation parametrized by $\omega$
	$f : \mathcal{X} \rightarrow \mathbb{R}^E$	Feature extractor
	$\gamma : \Omega \rightarrow \mathbb{R}^G$	Augmentation encoder
	$\pi : \mathbb{R}^{E+G} \rightarrow \mathbb{R}^k$	Projector
	$\mathcal{L} : \mathbb{R}^k \times \mathbb{R}^k \rightarrow \mathbb{R}$	Objective function in joint-embedding learning
<b>Dimensions</b>	$D$	Image shape, i.e. $D = 224 \times 224 \times 3$
	$A$	Augmentation vector size – depends on the choice of augmentations; in our case, $A = 14$ (see Section 3.3)
	$E$	Feature extractor embedding size – depends on the architecture; e.g. for Resnet-50 [34], $E = 2048$
	$G$	Augmentation encoder embedding size – hyperparameter; in our case, $G = 64$
	$k$	Projector embedding size – depends on the SSL method; e.g. for MoCo-v2, $k = 128$ (see Table 5)

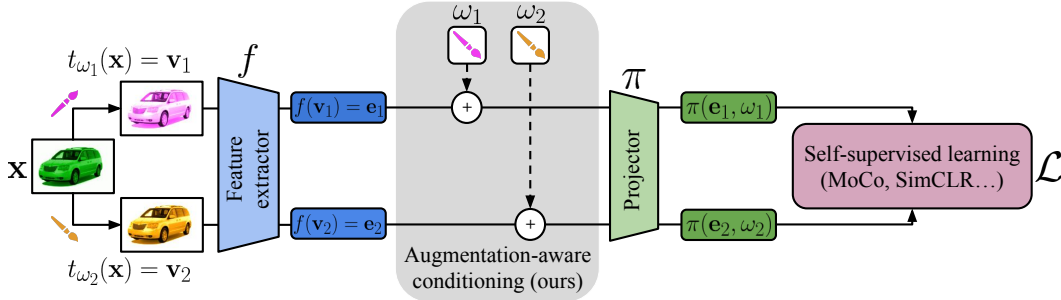


Figure 2: Overview of CASSLE. We extend the typical self-supervised learning approaches by incorporating the information of augmentations applied to images into the projector network. In CASSLE, the SSL objective is thus imposed on joint representations of images and the augmentations that had been applied to them. This way, CASSLE enables the feature extractor to be more aware of augmentations than the methods that do not condition the projector network.

### 3.1 Preliminaries

In this section, we introduce the key concepts in joint-embedding SSL. We include Table 1 as a reference of key concepts used in this manuscript. A typical joint-embedding framework used in self-supervised learning consists of an augmentation function  $t_\omega$  and two networks: feature extractor  $f$  and projector  $\pi$ . Let  $\mathbf{v}_1 = t_{\omega_1}(\mathbf{x})$ ,  $\mathbf{v}_2 = t_{\omega_2}(\mathbf{x})$  be two augmentations of a sample  $\mathbf{x} \sim \mathcal{X}$  parameterized by  $\omega_1, \omega_2 \sim \Omega$ . The feature extractor maps them into the embedding space, i.e. the representation used in downstream tasks. To make the representation invariant to data augmentations,  $\mathbf{e}_1 = f(\mathbf{v}_1)$  is forced to be similar to  $\mathbf{e}_2 = f(\mathbf{v}_2)$ . This can be expressed by various objective functions [26], such as contrastive InfoNCE [62, 14, 33]<sup>3</sup>, or CCA [71] – which we collectively denote as  $\mathcal{L}$ . Instead of imposing the objective  $\mathcal{L}$  directly on the embedding space of  $f$ , a projector  $\pi$  transforms the embeddings into another representation space, where  $\mathcal{L}$  is applied. This trick, known as *Guillotine Regularization*, helps the feature extractor to better generalize to downstream tasks, due to  $f$  not being directly affected by  $\mathcal{L}$  [70, 14, 16, 8].

Minimizing  $\mathcal{L}(\pi(\mathbf{e}_1), \pi(\mathbf{e}_2))$  directly leads to reducing the distance between embeddings  $\pi(\mathbf{e}_1)$  and  $\pi(\mathbf{e}_2)$ . However,  $\mathcal{L}$  still indirectly encourages the intermediate network representations (including the output of the feature extractor  $f$ ) to also conform to the objective to some extent. As a result, the feature extractor tends to erase the information about augmentation from its output representation. This behavior may however be detrimental for certain downstream tasks (see Figures 1 and 6), which rely on features affected by augmentations. For instance, learning invariance to color jittering through standard contrastive methods may lead to degraded performance on the downstream task of flower recognition, which is not a color-invariant task [60, 67]. Thus, the success of typical SSL approaches depends critically on a careful choice of augmentations used for model pretraining [14, 60].

### 3.2 CASSLE

We have reviewed Self-supervised learning (SSL) and the limitations of joint-embedding approaches. To overcome the above limitations, we facilitate the feature extractor to encode the information about augmentations in its output representation. In consequence, the obtained representation will be more informative for downstream tasks that depend on features modified by augmentations.

CASSLE achieves this goal by conditioning the projector  $\pi$  on the parameters of augmentations used to perturb the input image. Specifically, we modify  $\pi$  so that apart from embedding  $\mathbf{e}$ , it also receives augmentation information  $\omega$  and projects their joint representation into the space where the objective  $\mathcal{L}$  is imposed. We do not alter the  $\mathcal{L}$  itself; instead, training relies on minimizing the contrastive loss  $\mathcal{L}$  between  $\pi(\mathbf{e}_1|\omega_1)$  and  $\pi(\mathbf{e}_2|\omega_2)$ . Thus,  $\pi$  learns to draw  $\mathbf{e}_1$  and  $\mathbf{e}_2$  together in its representation space *on condition of  $\omega_1$  and  $\omega_2$* . We visualize the architecture of CASSLE in Figure 2.

<sup>3</sup>While contrastive objectives such as InfoNCE [62] regularize the representation using negative pairs, we omit them from our notation for the sake of brevity.

We provide a rationale for why CASSLE preserves information about augmented features in the representation space. Since augmentation information vectors  $\omega$  do not carry any information about source images  $\mathbf{x}$ , their usefulness during pretraining could be explained only by using knowledge of transformations  $t_\omega$  that had been applied to  $\mathbf{x}$  to form views  $\mathbf{v}$ . However, for such knowledge to be acted upon, features affected by  $t_\omega$  must be preserved in the feature extractor representation  $f(\mathbf{v})$ .

Let us assume the opposite, that  $\omega$  is not useful for CASSLE to solve the task defined by  $\mathcal{L}$ . If this were the case, then for any  $\omega_3 \sim \Omega$  the following would hold:

$$p(\pi(\mathbf{e}_1|\omega_1)|\pi(\mathbf{e}_2|\omega_2)) = p(\pi(\mathbf{e}_1|\omega_1)|\pi(\mathbf{e}_2|\omega_3)). \quad (1)$$

$p(\pi(\mathbf{e}_1|\omega_1)|\pi(\mathbf{e}_2|\omega_2))$  can be understood as conditional probability that  $\pi(\mathbf{e}_1|\omega_1)$  is a representation of an image  $\mathbf{x}$  transformed by  $t_{\omega_1}$ , given the knowledge that  $\pi(\mathbf{e}_2|\omega_2)$  is a representation of  $\mathbf{x}$  transformed by  $t_{\omega_2}$ . Equation 1 implies that replacing the knowledge of  $t_{\omega_2}$  with any other randomly sampled  $t_{\omega_3}$  does not affect the inference process of CASSLE.

To demonstrate that this is not the case, we measure in Figure 3 the cosine similarity (denoted as  $sim$ ;  $sim(\mathbf{a}, \mathbf{b}) = \frac{\mathbf{a}^\top \mathbf{b}}{\|\mathbf{a}\| \|\mathbf{b}\|}$ ) of projector representations of 5000 positive augmented image pairs from the ImageNet-100 test set, using a model trained with CASSLE. The green plot denotes the similarities

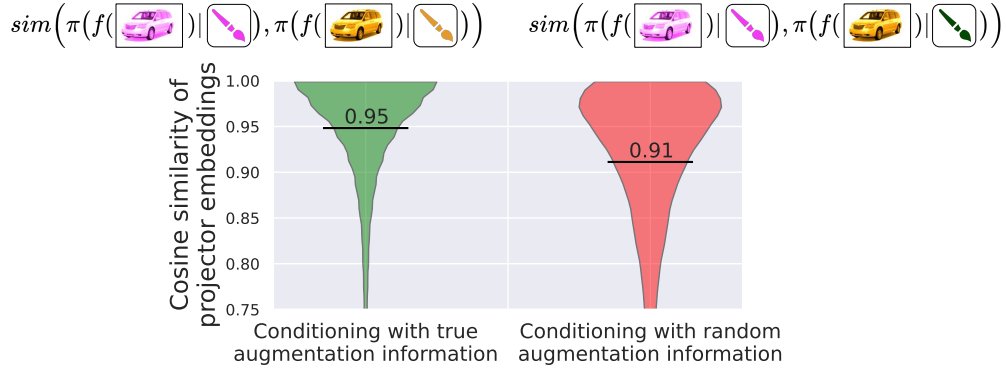


Figure 3: Cosine similarities of CASSLE projector ( $\pi$ ) representations when conditioned with augmentation information from either their respective images (green) or randomly sampled (red). Solid lines denote the mean values of similarities. Conditioning the CASSLE projector with wrong augmentation information decreases its ability to draw image pairs together, indicating that it indeed relies on augmentation information to perform its task.

of representations conditioned on the parameters of the augmentations used to construct those image pairs. On the other hand, in the red plot, one of the projector representations is conditioned with *false* augmentation parameters, i.e. randomly sampled parameters that are unrelated to the augmented image.

It is evident from Figure 3 that the cosine similarity of embeddings decreases when false augmentation parameters ( $\omega_3$  instead of  $\omega_2$ ) are supplied to the projector, i.e.:

$$\mathbb{E}_{x \sim \mathbb{X}, \{\omega_1, \omega_2, \omega_3\} \sim \Omega} [sim(\pi(\mathbf{e}_1|\omega_1), \pi(\mathbf{e}_2|\omega_2)) - sim(\pi(\mathbf{e}_1|\omega_1), \pi(\mathbf{e}_2|\omega_3))] > 0. \quad (2)$$

Recall that in contrastive SSL, the cosine similarity of embeddings corresponds to their probability density. This is because the InfoNCE loss is formulated as cross-entropy, where the activation function is defined as cosine similarity between respective image embeddings, and class labels are replaced with the indices of corresponding positive embedding pairs [62, 33, 14]. Hence, minimizing  $\mathcal{L}$  leads to:

$$sim(\pi(\mathbf{e}_1|\omega_1), \pi(\mathbf{e}_2|\omega_2)) \propto \frac{p(\pi(\mathbf{e}_1|\omega_1)|\pi(\mathbf{e}_2|\omega_2))}{p(\pi(\mathbf{e}_1|\omega_1))}. \quad (3)$$

It follows from 2 that, in practice

$$\mathbb{E}_{x \sim \mathbb{X}, \{\omega_1, \omega_2, \omega_3\} \sim \Omega} \left[ \frac{p(\pi(\mathbf{e}_1|\omega_1)|\pi(\mathbf{e}_2|\omega_2)) - p(\pi(\mathbf{e}_1|\omega_1)|\pi(\mathbf{e}_2|\omega_3))}{p(\pi(\mathbf{e}_1|\omega_1))} \right] > 0 \quad (4)$$

and, since  $p(\pi(\mathbf{e}_1|\omega_1)) > 0$ ,

$$\mathbb{E}_{x \sim \mathbb{X}, \{\omega_1, \omega_2, \omega_3\} \sim \Omega} [p(\pi(\mathbf{e}_1|\omega_1)|\pi(\mathbf{e}_2|\omega_2)) - p(\pi(\mathbf{e}_1|\omega_1)|\pi(\mathbf{e}_2|\omega_3))] > 0. \quad (5)$$

Moreover, we measure whether  $p(\pi(\mathbf{e}_1|\omega_1)|\pi(\mathbf{e}_2|\omega_2)) > p(\pi(\mathbf{e}_1|\omega_1)|\pi(\mathbf{e}_2|\omega_3))$  for each of the considered image view pairs and find it to be true in 92% of the considered cases.

In CASSLE, *the conditional probability of matching a positive pair of image representations increases when the correct augmentation information is known*, which implies that information describing the augmented features is indeed preserved in the representation of its feature extractor.

CASSLE can be applied to a variety of joint-embedding SSL methods, as the only practical modification it makes is changing the projector network to utilize the additional input  $\omega$ , describing the augmentations. We do not modify any other aspects of the self-supervised approaches, such as objective functions, which is appealing from a practical perspective. Last but not least, the architecture of the feature extractor in CASSLE is not affected by the introduced augmentation conditioning, as we only modify the input to the projector, which is discarded after the pretraining. Just like in vanilla SSL techniques, the feature extractor can be directly re-used for downstream tasks.

### 3.3 Practical implementation of the conditioning mechanism

We have introduced CASSLE and described the rationale behind this method. In this section, we discuss the practical aspects of the conditioning with augmentation information – the core component of CASSLE.

In this work, we focus on a set of augmentations used commonly in the literature [14, 16, 17], listed below along with descriptions of their respective parameters  $\omega^{aug}$ :

- **random cropping** –  $\omega^c \in [0, 1]^4$  describes the normalized coordinates of cropped image center and cropping sizes.
- **color jittering** –  $\omega^j \in [0, 1]^4$  describes the normalized intensities of brightness, contrast, saturation, and hue adjustment.
- **Gaussian blurring** –  $\omega^b \in [0, 1]$  is the standard deviation of the Gaussian filter used during the blurring operation.
- **random horizontal flipping** –  $\omega^f \in \{0, 1\}$  indicates whether the image has been flipped.
- **random grayscaling** –  $\omega^g \in \{0, 1\}$  indicates whether the image has been reduced to grayscale.

To enhance the projector’s awareness of the color changes in the augmented images, we additionally enrich  $\omega$  with information about **color difference** –  $\omega^d \in [0, 1]^3$ , which is computed as the difference between the mean values of color channels of the image before and after the color jittering operation. We empirically demonstrate that inclusion of  $\omega^d$  in  $\omega$  improves the performance of CASSLE (see Section 4.3).

We construct augmentation information  $\omega \in \Omega$  by concatenating vectors  $\omega^{aug}$  describing the parameters of each augmentation type [41]. Since each of the above  $\omega^{aug}$  can be expressed as a vector of one or more scalars, the concatenated augmentation information vectors contain 14 scalars, i.e.  $\omega \in \Omega \subset \mathbb{R}^{14}$ . We also explore withholding some augmentation information during training (resulting in an appropriately reduced size of  $\omega$ ), but find that conditioning on full augmentation information leads to the best representation quality (see Section 4.3).

We consider four methods of injecting  $\omega$  into  $\pi$ : joining  $\omega$  and  $\mathbf{e}$  through **(i)** concatenation, modulating  $\mathbf{e}$  with  $\omega$  through element-wise **(ii)** addition or **(iii)** multiplication, or **(iv)** using  $\omega$  as an input to a hypernetwork [31] which generates the parameters of  $\pi$ . Apart from concatenation, all of those methods require transforming  $\omega$  into *augmentation embeddings*  $\mathbf{g} \in \mathcal{G}$  of shapes required by the conditioning operation. For example, when modulating  $\mathbf{e}$  with  $\mathbf{g}$ , dimensions of  $\mathbf{e}$  and  $\mathbf{g}$  must be equal. For this purpose, we precede the projector with additional *Augmentation encoder*  $\gamma : \Omega \rightarrow \mathcal{G}$ . For the architecture of  $\gamma$  we choose the Multilayer Perceptron. An additional advantage of  $\gamma$  is that it allows for learning a representation of  $\omega$  which is more expressive for processing by  $\pi$ , which is typically a shallow network. We summarize the above conditioning mechanisms in Figure 4. In practice, we find that conditioning  $\pi$  through the concatenation of  $\mathbf{e}$  and  $\mathbf{g}$  yields the best-performing representation (see Section 4.3).

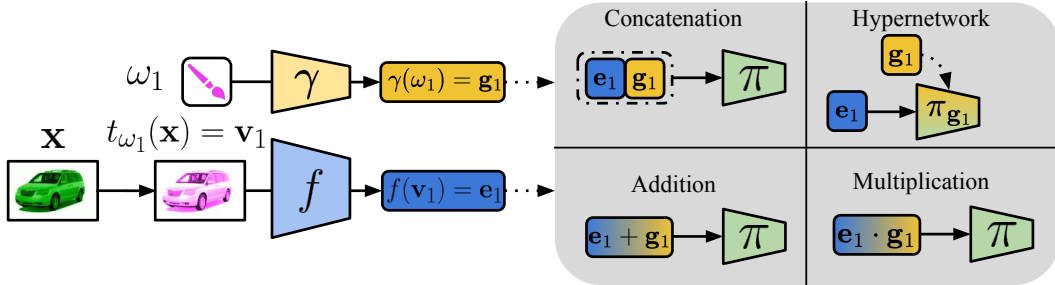


Figure 4: A visualization of four considered methods of conditioning the projector with augmentation information.

## 4 Experiments

We have introduced CASSLE and described the theoretical and practical aspects of its design. In this Section, we conduct an experimental analysis of our approach, which we use to extend several recent SSL frameworks – MoCo (Momentum Contrastive Learning) [33, 16, 18], SimCLR (Simple Framework for Contrastive Learning) [14], and Barlow Twins [71]. In Section 4.1, we evaluate CASSLE’s performance on downstream tasks such as classification, regression, object detection, and image retrieval<sup>4</sup>. In Section 4.2, we analyze the sensitivity to augmentations of representations formed by CASSLE. Next, we discuss the choice of hyperparameters of CASSLE in Section 4.3. Furthermore, we refer to B for a series of experiments that highlight several noteworthy features of CASSLE, including but not limited to its effect on the minimization of contrastive loss and generalizing to augmentations that were not observed during pretraining.

In all experiments, unless specified otherwise, we utilize the ResNet-50 architecture [34] and conduct the self-supervised pretraining on ImageNet-100 - a 100-class subset of the ILSVRC dataset [56] used commonly in the literature [60, 67, 41, 13]. We use the standard set of augmentations including horizontal flipping, random cropping, grayscaling, color jittering and Gaussian blurring [33, 41, 30]. For consistency in terms of hyperparameters, we follow [41] for MoCo-v2, and [13] for SimCLR. We refer to A for the details of pretraining, evaluation, and implementation.

### 4.1 Evaluation on downstream tasks

We begin the experimental analysis by addressing the most fundamental question – how does CASSLE impact the ability of models to generalize to downstream tasks? To answer it, we evaluate models pretrained via CASSLE and other self-supervised techniques on a variety of downstream visual tasks, such as classification, regression, object detection, and image retrieval.

**Linear evaluation** We evaluate the performance of pretrained networks on the downstream tasks of classification and regression on 13 different datasets typically used for evaluation of SSL methods [14, 41, 13], listed in Table 6. We follow the linear evaluation protocol [37, 14, 41], described in detail in A.2. We evaluate multiple self-supervised methods extended with CASSLE, as well as other recently proposed extensions which increase sensitivity to augmentations [41, 67, 13] or prevent feature suppression in SSL [55]. We report the full results in Table 2. We find that in the vast majority of cases, CASSLE improves the performance of vanilla joint-embedding methods, as well as other SSL extensions that foster augmentation sensitivity [41, 13].

**Object detection** We next evaluate the pretrained networks on a more challenging task of object detection on the VOC (Visual Object Classification) 2007 dataset [24]. We follow the training scheme of [33, 16], except that we only train the object detector modules and keep the feature extractor parameters fixed during training for detection to better compare the pretrained representations. We report the Average Precision (AP) [42] of models pretrained through MoCo-v2 and SimCLR [14] with AugSelf [41] and CASSLE extensions in Table 3. The compared approaches yield similar results, with CASSLE representation surpassing the vanilla methods and AugSelf.

<sup>4</sup>We compare CASSLE to several recently proposed methods and report their performance from the literature [67, 41, 13], given that the code for [67] was not made available at the time of writing. As for the results of baseline SSL models and AugSelf [41], we report their results from the literature except when our runs of those methods yielded results different by at least 2 pp. We mark such cases with †.



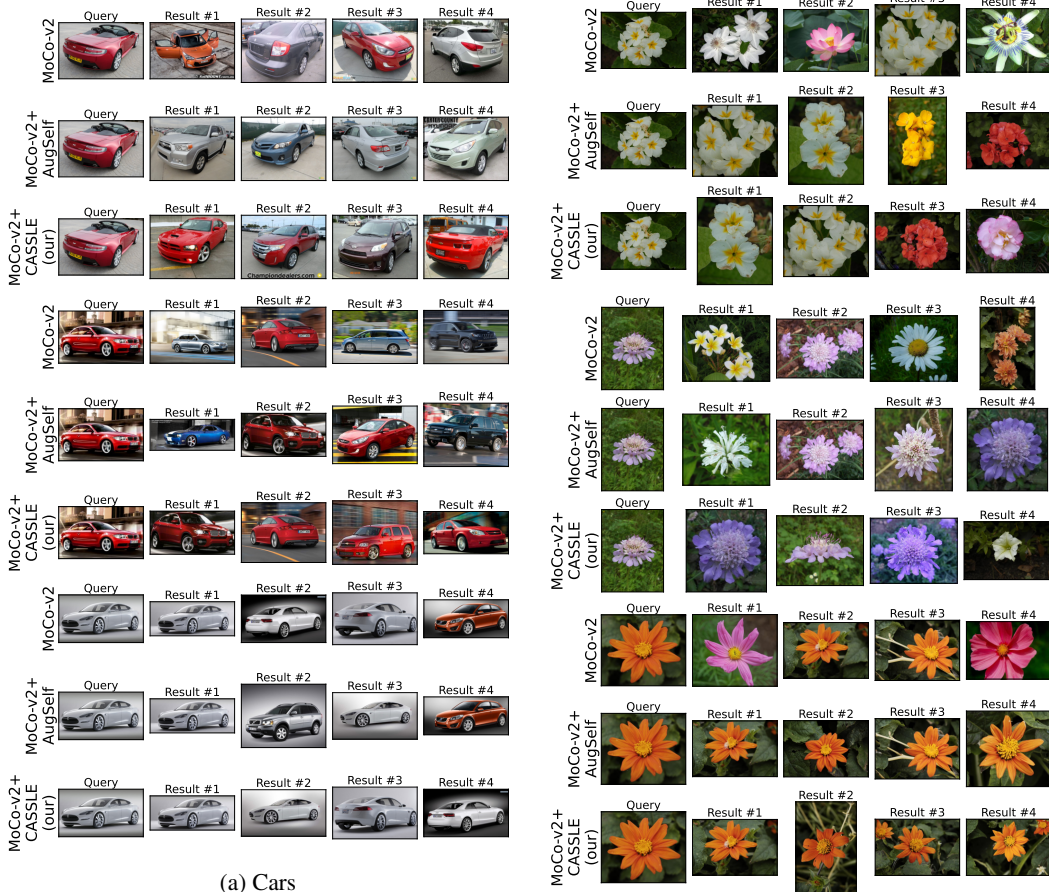
Table 2: Linear evaluation on downstream classification and regression tasks. CASSLE consistently improves representations formed by vanilla SSL approaches and performs better or comparably to other techniques of increasing sensitivity to augmentations [67, 41, 13].

Method	C10	C100	Food	MIT	Pets	Flowers	Caltech	Cars	FGVCA	DTD	SUN	CUB	300W
<i>SimCLR</i> [14]													
Vanilla	84.41 <sup>†</sup>	61.40	57.48 <sup>†</sup>	63.10 <sup>†</sup>	71.60 <sup>†</sup>	83.37 <sup>†</sup>	<b>79.67<sup>†</sup></b>	35.14 <sup>†</sup>	40.03 <sup>†</sup>	64.90	46.92 <sup>†</sup>	30.98 <sup>†</sup>	88.59 <sup>†</sup>
AugSelf [41] <sup>†</sup>	84.45	62.67	59.96	63.21	70.61	<b>85.77</b>	77.78	37.38	42.86	65.53	<b>49.18</b>	34.24	88.27
AI [13]	83.90	63.10	–	–	69.50	68.30	74.20	–	–	53.70	–	<b>38.60</b>	88.00
<b>CASSLE</b>	<b>86.31</b>	<b>64.36</b>	<b>60.67</b>	<b>63.96</b>	<b>72.33</b>	85.22	79.62	<b>39.86</b>	<b>43.10</b>	<b>65.96</b>	48.91	33.21	<b>88.88</b>
<i>MoCo-v2</i> [33, 16]													
Vanilla	84.60	61.60	59.67	61.64	70.08	82.43	77.25	33.86	41.21	64.47	46.50	32.20	88.77 <sup>†</sup>
AugSelf [41]	85.26	63.90	60.78	63.36	73.46	85.70	78.93	37.35	39.47	66.22	48.52	37.00	89.49 <sup>†</sup>
AI [13]	81.30	64.60	–	–	<b>74.00</b>	81.30	78.90	–	–	<b>68.80</b>	–	<b>41.40</b>	<b>90.00</b>
LooC [67]	–	–	–	–	–	–	–	–	–	–	39.60	–	–
IFM [55] <sup>†</sup>	83.36	60.22	59.86	60.60	72.99	85.73	78.77	36.54	41.05	62.34	47.48	35.90	88.92
<b>CASSLE</b>	<b>86.32</b>	<b>65.29</b>	<b>61.93</b>	<b>63.86</b>	72.86	<b>86.51</b>	<b>79.63</b>	<b>38.82</b>	<b>42.03</b>	66.54	<b>49.25</b>	36.22	88.93
<i>Barlow Twins</i> [71]													
Vanilla <sup>†</sup>	85.90	66.10	59.41	61.72	72.30	87.13	81.95	41.54	44.40	65.85	49.18	35.02	89.04
AugSelf [41] <sup>†</sup>	<b>87.28</b>	66.98	60.52	63.96	72.11	86.68	81.73	39.88	44.23	65.21	47.71	37.02	88.88
<b>CASSLE</b>	87.03	<b>67.27</b>	<b>62.19</b>	<b>65.08</b>	<b>72.75</b>	<b>87.99</b>	<b>82.56</b>	<b>41.68</b>	<b>46.63</b>	<b>66.31</b>	<b>50.09</b>	<b>38.25</b>	<b>89.52</b>
<i>MoCo-v3</i> [33, 18] with ViT-Small [22] pretrained on ImageNet-1K.													
Vanilla <sup>†</sup>	83.17	62.40	56.15	53.28	62.29	81.48	69.63	28.63	32.84	57.18	42.16	35.00	87.42
AugSelf [41] <sup>†</sup>	84.25	64.12	<b>58.28</b>	<b>56.12</b>	<b>63.93</b>	<b>83.13</b>	72.45	29.64	32.54	<b>60.27</b>	43.22	<b>37.16</b>	87.85
<b>CASSLE</b>	<b>85.13</b>	<b>64.67</b>	57.30	55.90	63.88	82.42	<b>73.53</b>	<b>30.92</b>	<b>35.91</b>	58.24	<b>43.37</b>	36.09	<b>88.53</b>

**Image retrieval** Finally, we evaluate the pre-trained models on the task of image retrieval. We gather the features of images from the Cars and Flowers test sets and for a given query image, select four images closest to it in terms of the cosine distance of final feature extractor representations. We compare the images retrieved by MoCo-v2, AugSelf [41] and CASSLE in Figure 5. CASSLE selects pictures of cars that are the most consistent in terms of color. In the case of flowers, the nearest neighbor retrieved by the vanilla model is a different species than that of the first query image, whereas both CASSLE and AugSelf select the first two nearest neighbors from the same species but then retrieve images of flowers with similar shapes, but different colors. This again indicates greater reliability of features learned by CASSLE. For subsequent queries, CASSLE and AugSelf retrieve in general more consistently looking images, in particular in terms of color scheme. This indicates a greater sensitivity of those models to shifts in colors.

Table 3: Average Precision of object detection on VOC dataset [24, 42]. CASSLE extension of MoCo-v2 and SimCLR outperforms the vanilla approaches and AugSelf extension by a small margin.

Method	<i>MoCo-v2</i> [33, 16]	<i>SimCLR</i> [14]
Vanilla	45.12	44.74
AugSelf [41]	45.20	44.50
<b>CASSLE</b>	<b>45.90</b>	<b>45.60</b>



(a) Cars

(b) Flowers

Figure 5: Image retrieval examples for Cars and Flowers datasets.

## 4.2 Analysis of representations formed by CASSLE

We have demonstrated that CASSLE has a positive impact on the quality of trained representations. We now investigate the differences in those representations. Specifically, we investigate the awareness of augmentation-induced data perturbations in the intermediate and final representations of pretrained networks. As a proxy metric for measuring this, we choose the InfoNCE loss [62, 14]. The value of InfoNCE is high if embeddings of pairs of augmented images are less similar to one another than to embeddings of other images, and low if positive embedding pairs are matched correctly, and thus, the given representation is invariant to augmentations. We report the mean InfoNCE loss values for different augmentation types at subsequent stages of ResNet-50 and projectors of vanilla MoCo-v2, AugSelf [41] and CASSLE in Figure 6.

In all networks, the augmentation awareness decreases gradually throughout the feature extractor and projector stages. In CASSLE, we observe a much softer decline in the feature extractor stages and a sharper one in the projector. Representations of CASSLE feature extractor are on average more difficult to match together than those of vanilla MoCo-v2 and AugSelf [41]. This implies that the CASSLE feature extractor is indeed more sensitive to augmentations than its counterparts. On the other hand, representations of all projectors, including CASSLE, are similarly separable. This suggests that the conditioning mechanism helps CASSLE projector to better amortize the augmentation-induced differences between the embeddings produced by the feature extractor.

The above observations indicate that in the vanilla and (to a slightly lesser extent) AugSelf approaches, both the projector and the intermediate representations are enforced to be augmentation-invariant. On the other hand, in CASSLE, the task of augmentation invariance is solved to a larger degree by the projector, and to a smaller degree by the feature extractor, allowing it to be more augmentation-aware. As shown in Section 4.1, this sensitivity does not prevent the CASSLE feature extractor from achieving similar or better performance than its counterparts when transferred to downstream tasks.

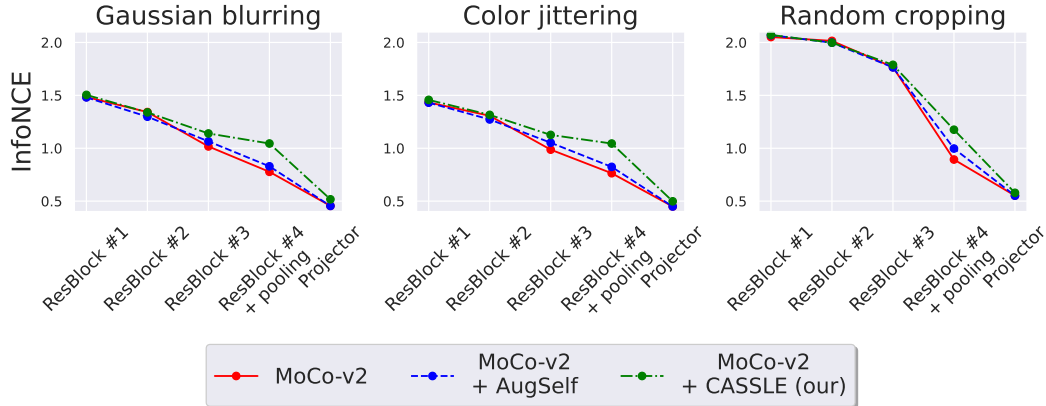


Figure 6: A comparison of InfoNCE loss measured on different kinds of augmentations at subsequent stages of the ResNet-50 and projectors pretrained by vanilla, AugSelf [41] and CASSLE variants of MoCo-v2. Feature extractor representation of CASSLE yields higher InfoNCE values which suggests that it is more susceptible to augmentations.

### 4.3 Ablation study

We have demonstrated the quality and properties of representations learned. We next examine the impact of different hyperparameters of CASSLE. We compare different variants of MoCo-v2+CASSLE on the same classification and regression tasks as in Section 4.1. We rank the models from best to worst performance on each task and report the average ranks in Table 4.

Table 4: Ablation study of CASSLE parameters. The results are computed with MoCo-v2+CASSLE. It is best to condition CASSLE on all available augmentation information. CASSLE yields the best results when implemented by concatenating or adding the augmentation and image embeddings together.

Parameter	C10	C100	Food	MIT	Pets	Flowers	Caltech	Cars	FGVCA	DTD	SUN	CUB	300W	Avg. rank ↓
Augmentation information contents														
$\omega^{\{c\}}$	84.89	62.95	59.74	63.96	72.26	83.55	79.66	38.78	42.03	65.11	48.44	33.86	89.17	4.54
$\omega^{\{c,j\}}$	85.56	64.26	60.35	62.61	71.97	84.73	79.86	38.13	42.17	66.28	48.01	34.24	88.76	4.54
$\omega^{\{c,j,d\}}$	85.87	63.91	61.07	63.51	72.71	86.53	79.51	38.27	42.53	66.70	49.27	35.76	89.11	3.00
$\omega^{\{c,j,b,f\}}$	86.16	64.51	60.80	63.81	72.83	84.66	79.90	38.93	43.02	66.12	48.96	34.40	88.69	2.84
$\omega^{\{c,j,b,f,g\}}$	85.85	64.14	61.24	63.73	72.88	84.50	79.93	38.23	41.28	65.27	48.90	34.47	88.78	3.53
$\omega^{\{c,j,b,f,g,d\}}$	86.99	65.28	61.83	63.51	73.22	86.55	79.87	37.97	41.70	67.18	48.85	36.92	89.03	<b>2.46</b>
Impact of utilizing color difference information during pretraining														
<b>CASSLE</b> $\omega^{\{c,j\}}$	85.56	64.26	60.35	62.61	71.97	84.73	79.86	38.13	42.17	66.28	48.01	34.24	88.76	4.53
<b>AugSelf</b> $\omega^{\{c,j\}}$	85.26	63.90	60.78	63.36	73.46	85.70	78.93	37.35	39.47	66.22	48.52	37.00	89.49	4.23
<b>CASSLE</b> $\omega^{\{c,j,d\}}$	85.87	63.91	61.07	63.51	72.71	86.53	79.51	38.27	42.53	66.70	49.27	35.76	89.11	2.76
<b>AugSelf</b> $\omega^{\{c,j,d\}}$	84.95	64.06	61.53	63.06	73.52	86.25	77.38	36.00	42.54	66.33	48.65	37.40	88.36	3.69
<b>CASSLE</b> $\omega^{\{c,j,b,f,g\}}$	85.85	64.14	61.24	63.73	72.88	84.50	79.93	38.23	41.28	65.27	48.90	34.47	88.78	3.46
<b>CASSLE</b> $\omega^{\{c,j,b,f,g,d\}}$	86.99	65.28	61.83	63.51	73.22	86.55	79.87	37.97	41.70	67.18	48.85	36.92	89.03	<b>2.23</b>
Method of conditioning the projector														
<b>Concatenation</b>	86.99	65.28	61.83	63.51	73.22	86.55	79.87	37.97	41.70	67.18	48.85	36.92	89.03	<b>1.92</b>
<b>Addition</b>	86.45	65.40	63.00	65.15	71.34	86.91	79.79	37.83	42.18	66.17	49.28	37.42	88.87	<b>1.92</b>
<b>Multiplication</b>	86.72	66.70	60.65	60.97	64.60	85.17	80.09	33.54	41.56	63.99	47.63	32.15	89.48	2.69
<b>Hypernetwork</b>	84.70	63.55	60.62	64.10	67.16	82.76	78.47	33.39	39.85	66.44	47.43	30.48	89.11	3.46
Depth of the Augmentation encoder (0 denotes concatenating raw $\omega$ to $e$ )														
<b>0</b>	86.53	65.99	62.54	61.72	69.04	85.46	80.74	36.44	41.91	65.64	48.55	33.88	92.72	3.38
<b>2</b>	86.57	64.80	61.85	62.68	72.79	86.31	79.93	37.85	42.87	66.32	49.23	35.39	88.86	3.08
<b>4</b>	86.32	65.16	61.98	64.93	72.64	86.49	79.75	38.64	41.46	66.91	49.71	36.56	89.27	2.38
<b>6</b>	86.99	65.28	61.83	63.51	73.22	86.55	79.87	37.97	41.70	67.18	48.85	36.92	89.03	<b>2.15</b>
<b>8</b>	85.47	64.88	61.49	63.13	72.41	85.65	78.22	37.82	40.71	66.70	49.21	36.09	88.90	4.00
Hidden size of the Augmentation encoder														
<b>16</b>	84.51	63.40	61.38	62.31	71.61	85.40	78.96	37.53	41.84	66.54	48.68	35.54	88.78	5.54
<b>32</b>	85.43	63.94	61.93	64.18	72.05	85.67	79.80	37.86	41.52	67.13	48.71	35.64	88.67	4.38
<b>64</b>	86.99	65.28	61.83	63.51	73.22	86.55	79.87	37.97	41.70	67.18	48.85	36.92	89.03	<b>2.54</b>
<b>128</b>	86.24	64.66	61.95	64.25	72.12	86.72	79.56	37.79	42.71	67.61	49.52	36.87	88.99	2.62
<b>256</b>	86.23	65.63	61.77	61.79	72.03	85.69	80.38	37.86	40.94	67.07	49.59	37.00	89.37	3.31
<b>512</b>	85.77	66.05	62.21	64.55	72.45	86.38	80.06	37.91	41.94	66.22	49.35	36.24	88.87	2.69

**Augmentation information contents** We compare conditioning the projector with different subsets of augmentation information<sup>5</sup> The average best representation is trained with conditioning on all possible augmentation information. Moreover, using the additional **color difference** ( $\omega^d$ ) information additionally improves the results, indicating that it is indeed useful to consider not only augmentation parameters but also information about its effects.

**Impact of utilizing color difference information** We verify that the improved performance of CASSLE does not stem solely from using augmentation information that has not been considered in prior works, i.e. color difference ( $\omega^d$ ). We compare a variant of AugSelf which learns to predict color difference values in addition to augmentation information used by [41], i.e. cropping ( $\omega^c$ ) and color jittering ( $\omega^j$ ), as well as a variant of CASSLE conditioned on all augmentation information *except*  $\omega^d$  (i.e.  $\omega^{\{c,j,b,f,g\}}$ ). We find that while including  $\omega^d$  improves the performance of AugSelf and CASSLE, both variants of CASSLE achieve better results than both variants of AugSelf. We also compare variants CASSLE conditioned with the same parameters as used with AugSelf, i.e.  $\omega^{\{c,j\}}$  and  $\omega^{\{c,j,d\}}$ . Models that use only the jittering and cropping information ( $\omega^{\{c,j\}}$ ) perform similarly, achieving the mean ranks of 4.53 and 4.23. In the case of  $\omega^{\{c,j,d\}}$ , CASSLE and AugSelf differ by a larger margin, achieving the mean rank of 2.76, and 3.69 respectively. The above results underscore the usefulness of using all available augmentation parameters, including color difference, in CASSLE. In contrast, Lee et. al. [41] observe that predicting all augmentation parameters in AugSelf lowers the quality of the trained model.

**Method of conditioning the projector** We compare conditioning the projector through (i) concatenation, element-wise (ii) addition or (iii) multiplication, or (iv) using augmentation information as an input to a hypernetwork [31] which generates the parameters of  $\pi$ . Conditioning through **concatenation** and **addition** yields on average the strongest performance on downstream tasks. We choose to utilize the **concatenation** method in our experiments, as it requires a slightly smaller Augmentation encoder.

**Size of the Augmentation encoder** While CASSLE is robust to the size of the  $\gamma$  MLP, using the depth and hidden size of 6 and 64, respectively, yields the strongest downstream performance. In particular, the variant of CASSLE that utilizes the Augmentation encoder performs better than the variant that concatenates  $\mathbf{e}$  to raw augmentation embeddings  $\omega$ . Given such an architecture of the Augmentation encoder, our computation overhead is negligible as we increase the overall number of parameters by around 0.1% compared to vanilla SSL approaches.

## 5 Conclusion

In this paper, we propose CASSLE: a novel method for augmentation-aware self-supervised learning that retains information about data augmentations in the representation space. To accomplish this, we introduce the concept of the conditioned projector, which receives augmentation information while processing the representation vector. Our solution necessitates only small architectural changes and no additional auxiliary loss components. Therefore, the training concentrates on contrastive loss, which enhances overall performance. We compare our solution with existing augmentation-aware SSL methods and demonstrate its superior performance on downstream tasks, particularly when augmentation invariance leads to the loss of vital information. Moreover, we show that it obtains representations more sensitive to augmentations than the baseline methods. Overall, our method offers a straightforward and efficient approach to retaining information about data augmentations in the representation space. It can be directly applied to SSL methods, contributing to the further advancement of augmentation-aware self-supervised learning.

---

<sup>5</sup>We recall the notation used for Augmentation information contents –  $\omega^{\{x,y\}}$  denotes including parameters of augmentations  $\{x, y\}$  in augmentation information vector  $\omega$ . For example,  $\omega^{\{c,j\}}$  denotes  $\omega$  containing cropping and color jittering parameters.

## Acknowledgments

This research has been supported by the flagship project entitled "Artificial Intelligence Computing Center Core Facility" from the Priority Research Area DigiWorld under the Strategic Programme Excellence Initiative at Jagiellonian University, and by the Horizon Europe Programme (HORIZON-CL4-2022-HUMAN-02) under the project "ELIAS: European Lighthouse of AI for Sustainability", GA no. 101120237. The research of Marcin Przewięźlikowski was supported by the National Science Centre (Poland), grant no. 2023/49/N/ST6/03268. The research of Marek Śmieja was supported by the National Science Centre (Poland), grant no. 2022/45/B/ST6/01117. The research of Bartosz Zieliński is funded in part by National Science Centre (Poland) grant number 2022/47/B/ST6/03397. Bartłomiej Twardowski acknowledges the grant RYC2021-032765-I. We gratefully acknowledge Polish high-performance computing infrastructure PLGrid (HPC Centers: ACK Cyfronet AGH) for providing computer facilities and support within computational grant no. PLG/2023/016303.

The authors would like to express their gratitude to Przemysław Spurek, Tomasz Trzciński, Maciej Wołczyk, Michał Zając, Marcin Sendera, Filip Szatkowski, and Daniel Marczak for the insightful discussions throughout the work. The authors would also like to thank Hankook Lee and Ruchika Chavhan for releasing the codebases of AugSelf and Amortised Invariance, which served as bases for the development of CASSLE.

## References

- [1] Saleh Albelwi. Survey on self-supervised learning: Auxiliary pretext tasks and contrastive learning methods in imaging. *Entropy*, 24(4), 2022.
- [2] Haoping Bai, Meng Cao, Ping Huang, and Jiulong Shan. Self-supervised semi-supervised learning for data labeling and quality evaluation. In *NeurIPS Workshop*, 2021.
- [3] Randall Balestriero, Mark Ibrahim, Vlad Sobal, Ari S. Morcos, Shashank Shekhar, Tom Goldstein, Florian Bordes, Adrien Bardes, Grégoire Mialon, Yuandong Tian, Avi Schwarzschild, Andrew Gordon Wilson, Jonas Geiping, Quentin Garrido, Pierre Fernandez, Amir Bar, Hamed Pirsiavash, Yann LeCun, and Micah Goldblum. A cookbook of self-supervised learning. *ArXiv*, abs/2304.12210, 2023.
- [4] Adrien Bardes, Jean Ponce, and Yann LeCun. VICReg: Variance-invariance-covariance regularization for self-supervised learning. In *International Conference on Learning Representations*, 2022.
- [5] Suzanna Becker and Geoffrey Hinton. Self-organizing neural network that discovers surfaces in random-dot stereograms. *Nature*, 355:161–3, 02 1992.
- [6] Javad Zolfaghari Bengar, Joost van de Weijer, Bartłomiej Twardowski, and Bogdan Raducanu. Reducing label effort: Self-supervised meets active learning. In *Proceedings of the IEEE/CVF International Conference on Computer Vision (ICCV) Workshops*, pages 1631–1639, October 2021.
- [7] Sangnie Bhardwaj, Willie McClinton, Tongzhou Wang, Guillaume Lajoie, Chen Sun, Phillip Isola, and Dilip Krishnan. Steerable equivariant representation learning, 2023.
- [8] Florian Bordes, Randall Balestriero, Quentin Garrido, Adrien Bardes, and Pascal Vincent. Guillotine regularization: Why removing layers is needed to improve generalization in self-supervised learning. *Transactions on Machine Learning Research*, 2023.
- [9] Lukas Bossard, Matthieu Guillaumin, and Luc Van Gool. Food-101 – mining discriminative components with random forests. In *European Conference on Computer Vision*, 2014.
- [10] Tom Brown, Benjamin Mann, Nick Ryder, Melanie Subbiah, Jared D Kaplan, Prafulla Dhariwal, Arvind Neelakantan, Pranav Shyam, Girish Sastry, Amanda Askell, et al. Language models are few-shot learners. volume 33, pages 1877–1901, 2020.
- [11] Mathilde Caron, Ishan Misra, Julien Mairal, Priya Goyal, Piotr Bojanowski, and Armand Joulin. Unsupervised learning of visual features by contrasting cluster assignments. In H. Larochelle, M. Ranzato, R. Hadsell, M.F. Balcan, and H. Lin, editors, *Advances in Neural Information Processing Systems*, volume 33, pages 9912–9924. Curran Associates, Inc., 2020.
- [12] Mathilde Caron, Hugo Touvron, Ishan Misra, Hervé Jégou, Julien Mairal, Piotr Bojanowski, and Armand Joulin. Emerging properties in self-supervised vision transformers. In *Proceedings of the International Conference on Computer Vision (ICCV)*, 2021.
- [13] Ruchika Chavhan, Jan Stuehmer, Calum Heggan, Mehrdad Yaghoobi, and Timothy Hospedales. Amortised invariance learning for contrastive self-supervision. In *The Eleventh International Conference on Learning Representations*, 2023.

- [14] Ting Chen, Simon Kornblith, Mohammad Norouzi, and Geoffrey Hinton. A simple framework for contrastive learning of visual representations. In Hal Daumé III and Aarti Singh, editors, *Proceedings of the 37th International Conference on Machine Learning*, volume 119 of *Proceedings of Machine Learning Research*, pages 1597–1607. PMLR, 13–18 Jul 2020.
- [15] Ting Chen, Calvin Luo, and Lala Li. Intriguing properties of contrastive losses. In A. Beygelzimer, Y. Dauphin, P. Liang, and J. Wortman Vaughan, editors, *Advances in Neural Information Processing Systems*, 2021.
- [16] Xinlei Chen, Haoqi Fan, Ross B. Girshick, and Kaiming He. Improved baselines with momentum contrastive learning. *CoRR*, abs/2003.04297, 2020.
- [17] Xinlei Chen and Kaiming He. Exploring simple siamese representation learning. In *Proceedings of the IEEE/CVF Conference on Computer Vision and Pattern Recognition (CVPR)*, pages 15750–15758, June 2021.
- [18] Xinlei Chen, Saining Xie, and Kaiming He. An empirical study of training self-supervised vision transformers. In *Proceedings of the IEEE/CVF International Conference on Computer Vision (ICCV)*, pages 9640–9649, October 2021.
- [19] M. Cimpoi, S. Maji, I. Kokkinos, S. Mohamed, , and A. Vedaldi. Describing textures in the wild. In *Proceedings of the IEEE Conf. on Computer Vision and Pattern Recognition (CVPR)*, 2014.
- [20] Jacob Devlin, Ming-Wei Chang, Kenton Lee, and Kristina Toutanova. BERT: Pre-training of deep bidirectional transformers for language understanding, June 2019.
- [21] Carl Doersch, Abhinav Gupta, and Alexei A. Efros. Unsupervised visual representation learning by context prediction. In *Proceedings of the IEEE International Conference on Computer Vision (ICCV)*, December 2015.
- [22] Alexey Dosovitskiy, Lucas Beyer, Alexander Kolesnikov, Dirk Weissenborn, Xiaohua Zhai, Thomas Unterthiner, Mostafa Dehghani, Matthias Minderer, Georg Heigold, Sylvain Gelly, Jakob Uszkoreit, and Neil Houlsby. An image is worth 16x16 words: Transformers for image recognition at scale. In *International Conference on Learning Representations*, 2021.
- [23] Linus Ericsson, Henry Gouk, and Timothy Hospedales. Why do self-supervised models transfer? on the impact of invariance on downstream tasks. In *33rd British Machine Vision Conference 2022, BMVC 2022, London, UK, November 21-24, 2022*. BMVA Press, 2022.
- [24] M. Everingham, L. Van Gool, C. K. I. Williams, J. Winn, and A. Zisserman. The PASCAL Visual Object Classes Challenge 2007 (VOC2007) Results. <http://www.pascal-network.org/challenges/VOC/voc2007/workshop/index.html>.
- [25] Li Fei-Fei, R. Fergus, and P. Perona. One-shot learning of object categories. *IEEE Transactions on Pattern Analysis and Machine Intelligence*, 28(4):594–611, 2006.
- [26] Quentin Garrido, Yubei Chen, Adrien Bardes, Laurent Najman, and Yann Lecun. On the duality between contrastive and non-contrastive self-supervised learning. 2022.
- [27] Quentin Garrido, Laurent Najman, and Yann Lecun. Self-supervised learning of split invariant equivariant representations. In Andreas Krause, Emma Brunskill, Kyunghyun Cho, Barbara Engelhardt, Sivan Sabato, and Jonathan Scarlett, editors, *Proceedings of the 40th International Conference on Machine Learning*, volume 202 of *Proceedings of Machine Learning Research*, pages 10975–10996. PMLR, 23–29 Jul 2023.
- [28] Spyros Gidaris, Praveer Singh, and Nikos Komodakis. Unsupervised representation learning by predicting image rotations. In *International Conference on Learning Representations*, 2018.
- [29] Ian Goodfellow, Yoshua Bengio, and Aaron Courville. *Deep learning*. MIT press, 2016.
- [30] Jean-Bastien Grill, Florian Strub, Florent Altché, Corentin Tallec, Pierre Richemond, Elena Buchatskaya, Carl Doersch, Bernardo Avila Pires, Zhaohan Guo, Mohammad Gheshlaghi Azar, Bilal Piot, koray kavukcuoglu, Remi Munos, and Michal Valko. Bootstrap your own latent - a new approach to self-supervised learning. In H. Larochelle, M. Ranzato, R. Hadsell, M.F. Balcan, and H. Lin, editors, *Advances in Neural Information Processing Systems*, volume 33, pages 21271–21284. Curran Associates, Inc., 2020.
- [31] David Ha, Andrew M. Dai, and Quoc V. Le. Hypernetworks. In *International Conference on Learning Representations*, 2017.
- [32] Kaiming He, Xinlei Chen, Saining Xie, Yanghao Li, Piotr Dollár, and Ross Girshick. Masked autoencoders are scalable vision learners. In *Proceedings of the IEEE/CVF Conference on Computer Vision and Pattern Recognition (CVPR)*, pages 16000–16009, June 2022.
- [33] Kaiming He, Haoqi Fan, Yuxin Wu, Saining Xie, and Ross Girshick. Momentum contrast for unsupervised visual representation learning. In *Proceedings of the IEEE/CVF Conference on Computer Vision and Pattern Recognition (CVPR)*, June 2020.

- [34] Kaiming He, Xiangyu Zhang, Shaoqing Ren, and Jian Sun. Deep residual learning for image recognition. In *Proceedings of the IEEE Conference on Computer Vision and Pattern Recognition (CVPR)*, June 2016.
- [35] Dan Hendrycks and Thomas Dietterich. Benchmarking neural network robustness to common corruptions and perturbations. In *International Conference on Learning Representations*, 2019.
- [36] Tae Soo Kim, Geonwoon Jang, Sanghyup Lee, and Thijs Kooi. Did you get what you paid for? rethinking annotation cost of deep learning based computer aided detection in chest radiographs. In Linwei Wang, Qi Dou, P. Thomas Fletcher, Stefanie Speidel, and Shuo Li, editors, *Medical Image Computing and Computer Assisted Intervention – MICCAI 2022*, pages 261–270, Cham, 2022. Springer Nature Switzerland.
- [37] Simon Kornblith, Jonathon Shlens, and Quoc V. Le. Do better imagenet models transfer better? In *Proceedings of the IEEE/CVF Conference on Computer Vision and Pattern Recognition (CVPR)*, June 2019.
- [38] Jonathan Krause, Michael Stark, Jia Deng, and Li Fei-Fei. 3d object representations for fine-grained categorization. In *4th International IEEE Workshop on 3D Representation and Recognition (3dRR-13)*, Sydney, Australia, 2013.
- [39] Alex Krizhevsky. Learning multiple layers of features from tiny images. 2009.
- [40] Amit Krishan Kumar, M. Ritam, Lina Han, Shuli Guo, and Rohitash Chandra. Deep learning for predicting respiratory rate from biosignals. *Computers in Biology and Medicine*, 144:105338, 2022.
- [41] Hankook Lee, Kibok Lee, Kimin Lee, Honglak Lee, and Jinwoo Shin. Improving transferability of representations via augmentation-aware self-supervision. In M. Ranzato, A. Beygelzimer, Y. Dauphin, P.S. Liang, and J. Wortman Vaughan, editors, *Advances in Neural Information Processing Systems*, volume 34, pages 17710–17722. Curran Associates, Inc., 2021.
- [42] Tsung-Yi Lin, Michael Maire, Serge J. Belongie, Lubomir D. Bourdev, Ross B. Girshick, James Hays, Pietro Perona, Deva Ramanan, Piotr Dollár, and C. Lawrence Zitnick. Microsoft COCO: common objects in context. *CoRR*, abs/1405.0312, 2014.
- [43] Subhransu Maji, Esa Rahtu, Juho Kannala, Matthew B. Blaschko, and Andrea Vedaldi. Fine-grained visual classification of aircraft. *CoRR*, abs/1306.5151, 2013.
- [44] Grégoire Mialon, Randall Balestriero, and Yann LeCun. Variance covariance regularization enforces pairwise independence in self-supervised representations, 2023.
- [45] Volodymyr Mnih, Koray Kavukcuoglu, David Silver, Andrei A Rusu, Joel Veness, Marc G Bellemare, Alex Graves, Martin Riedmiller, Andreas K Fidjeland, Georg Ostrovski, et al. Human-level control through deep reinforcement learning. *nature*, 518(7540):529–533, 2015.
- [46] Maria-Elena Nilsback and Andrew Zisserman. Automated flower classification over a large number of classes. In *Indian Conference on Computer Vision, Graphics and Image Processing*, Dec 2008.
- [47] Mehdi Noroozi and Paolo Favaro. Unsupervised learning of visual representations by solving jigsaw puzzles. In Bastian Leibe, Jiri Matas, Nicu Sebe, and Max Welling, editors, *Computer Vision – ECCV 2016*, pages 69–84, Cham, 2016. Springer International Publishing.
- [48] Maxime Oquab, Timothée Darcet, Théo Moutakanni, Huy Vo, Marc Szafraniec, Vasil Khalidov, Pierre Fernandez, Daniel Haziza, Francisco Massa, Alaaeldin El-Nouby, Mahmoud Assran, Nicolas Ballas, Wojciech Galuba, Russell Howes, Po-Yao Huang, Shang-Wen Li, Ishan Misra, Michael Rabbat, Vasu Sharma, Gabriel Synnaeve, Hu Xu, Hervé Jegou, Julien Mairal, Patrick Labatut, Armand Joulin, and Piotr Bojanowski. Dinov2: Learning robust visual features without supervision. *ArXiv*, abs/2304.07193, 2023.
- [49] Utku Ozbulak, Hyun Jung Lee, Beril Boga, Esla Timothy Anzaku, Ho min Park, Arnout Van Messem, Wesley De Neve, and Joris Vankerschaver. Know your self-supervised learning: A survey on image-based generative and discriminative training. *Transactions on Machine Learning Research*, 2023. Survey Certification.
- [50] Omkar M. Parkhi, Andrea Vedaldi, Andrew Zisserman, and C. V. Jawahar. Cats and dogs. In *IEEE Conference on Computer Vision and Pattern Recognition*, 2012.
- [51] Adam Paszke, Sam Gross, Francisco Massa, Adam Lerer, James Bradbury, Gregory Chanan, Trevor Killeen, Zeming Lin, Natalia Gimelshein, Luca Antiga, Alban Desmaison, Andreas Kopf, Edward Yang, Zachary DeVito, Martin Raison, Alykhan Tejani, Sasank Chilamkurthy, Benoit Steiner, Lu Fang, Junjie Bai, and Soumith Chintala. Pytorch: An imperative style, high-performance deep learning library. In *Advances in Neural Information Processing Systems 32*, pages 8024–8035. Curran Associates, Inc., 2019.
- [52] Ariadna Quattoni and Antonio Torralba. Recognizing indoor scenes. In *2009 IEEE Conference on Computer Vision and Pattern Recognition*, pages 413–420, 2009.
- [53] Aniruddh Raghu, Jonathan Lorraine, Simon Kornblith, Matthew McDermott, and David K Duvenaud. Meta-learning to improve pre-training. In M. Ranzato, A. Beygelzimer, Y. Dauphin, P.S. Liang, and J. Wortman Vaughan, editors, *Advances in Neural Information Processing Systems*, volume 34, pages 23231–23244. Curran Associates, Inc., 2021.

- [54] Shaoqing Ren, Kaiming He, Ross Girshick, and Jian Sun. Faster r-cnn: Towards real-time object detection with region proposal networks. In C. Cortes, N. Lawrence, D. Lee, M. Sugiyama, and R. Garnett, editors, *Advances in Neural Information Processing Systems*, volume 28. Curran Associates, Inc., 2015.
- [55] Joshua Robinson, Li Sun, Ke Yu, Kayhan Batmanghelich, Stefanie Jegelka, and Suvrit Sra. Can contrastive learning avoid shortcut solutions? In M. Ranzato, A. Beygelzimer, Y. Dauphin, P.S. Liang, and J. Wortman Vaughan, editors, *Advances in Neural Information Processing Systems*, volume 34, pages 4974–4986. Curran Associates, Inc., 2021.
- [56] Olga Russakovsky, Jia Deng, Hao Su, Jonathan Krause, Sanjeev Satheesh, Sean Ma, Zhiheng Huang, Andrej Karpathy, Aditya Khosla, Michael Bernstein, Alexander Berg, and Li Fei-Fei. Imagenet large scale visual recognition challenge. *International Journal of Computer Vision*, 115, 09 2014.
- [57] C. Sagonas, E. Antonakos, Tzimiropoulos G, S. Zafeiriou, and M. Pantic. 300 faces in-the-wild challenge: Database and results. In *Image and Vision Computing (IMAVIS), Special Issue on Facial Landmark Localisation*, 2016.
- [58] Madeline C. Schiappa, Yogesh S. Rawat, and Mubarak Shah. Self-supervised learning for videos: A survey. *ACM Computing Surveys*, dec 2022.
- [59] Keyu Tian, Yi Jiang, qishuai diao, Chen Lin, Liwei Wang, and Zehuan Yuan. Designing BERT for convolutional networks: Sparse and hierarchical masked modeling. In *The Eleventh International Conference on Learning Representations*, 2023.
- [60] Yonglong Tian, Chen Sun, Ben Poole, Dilip Krishnan, Cordelia Schmid, and Phillip Isola. What makes for good views for contrastive learning? 33:6827–6839, 2020.
- [61] Yuandong Tian. Understanding deep contrastive learning via coordinate-wise optimization. In Alice H. Oh, Alekh Agarwal, Danielle Belgrave, and Kyunghyun Cho, editors, *Advances in Neural Information Processing Systems*, 2022.
- [62] Aäron van den Oord, Yazhe Li, and Oriol Vinyals. Representation learning with contrastive predictive coding. *CoRR*, abs/1807.03748, 2018.
- [63] Diane Wagner, Fabio Ferreira, Danny Stoll, Robin Tibor Schirrmeyer, Samuel Müller, and Frank Hutter. On the importance of hyperparameters and data augmentation for self-supervised learning. In *First Workshop on Pre-training: Perspectives, Pitfalls, and Paths Forward at ICML 2022*, 2022.
- [64] C. Wah, S. Branson, P. Welinder, P. Perona, and S. Belongie. The Caltech-UCSD Birds-200-2011 Dataset. Technical Report CNS-TR-2011-001, California Institute of Technology, 2011.
- [65] Kristoffer Wickstrøm, Michael Kampffmeyer, Karl Øyvind Mikalsen, and Robert Jenssen. Mixing up contrastive learning: Self-supervised representation learning for time series. *Pattern Recognition Letters*, 155:54–61, mar 2022.
- [66] J. Xiao, J. Hays, K. A. Ehinger, A. Oliva, and A. Torralba. Sun database: Large-scale scene recognition from abbey to zoo. In *2010 IEEE Computer Society Conference on Computer Vision and Pattern Recognition*, pages 3485–3492, June 2010.
- [67] Tete Xiao, Xiaolong Wang, Alexei A Efros, and Trevor Darrell. What should not be contrastive in contrastive learning. In *International Conference on Learning Representations*, 2021.
- [68] Yuyang Xie, Jianhong Wen, Kin Wai Lau, Yasar Abbas Ur Rehman, and Jiajun Shen. What should be equivariant in self-supervised learning. In *Proceedings of the IEEE/CVF Conference on Computer Vision and Pattern Recognition (CVPR) Workshops*, pages 4111–4120, June 2022.
- [69] Zhenda Xie, Zheng Zhang, Yue Cao, Yutong Lin, Jianmin Bao, Zhuliang Yao, Qi Dai, and Han Hu. Simsim: A simple framework for masked image modeling. In *Proceedings of the IEEE/CVF Conference on Computer Vision and Pattern Recognition (CVPR)*, pages 9653–9663, June 2022.
- [70] Jason Yosinski, Jeff Clune, Yoshua Bengio, and Hod Lipson. How transferable are features in deep neural networks? In Z. Ghahramani, M. Welling, C. Cortes, N. Lawrence, and K.Q. Weinberger, editors, *Advances in Neural Information Processing Systems*, volume 27. Curran Associates, Inc., 2014.
- [71] Jure Zbontar, Li Jing, Ishan Misra, Yann LeCun, and Stephane Deny. Barlow twins: Self-supervised learning via redundancy reduction. In Marina Meila and Tong Zhang, editors, *Proceedings of the 38th International Conference on Machine Learning*, volume 139 of *Proceedings of Machine Learning Research*, pages 12310–12320. PMLR, 18–24 Jul 2021.
- [72] Liheng Zhang, Guo-Jun Qi, Liqiang Wang, and Jiebo Luo. Aet vs. aed: Unsupervised representation learning by auto-encoding transformations rather than data. In *Proceedings of the IEEE/CVF Conference on Computer Vision and Pattern Recognition (CVPR)*, June 2019.
- [73] Richard Zhang, Phillip Isola, and Alexei A. Efros. Colorful image colorization. In Bastian Leibe, Jiri Matas, Nicu Sebe, and Max Welling, editors, *Computer Vision – ECCV 2016*, pages 649–666, Cham, 2016. Springer International Publishing.



- [74] Simone Zini, Alex Gomez-Villa, Marco Buzzelli, Bartłomiej Twardowski, Andrew D. Bagdanov, and Joost van de weijer. Planckian jitter: countering the color-crippling effects of color jitter on self-supervised training. In *The Eleventh International Conference on Learning Representations*, 2023.

## A Pretraining and evaluation details

In this section, we describe the details of Self-Supervised pretraining and the evaluation methodology used in our experiments.

### A.1 Pretraining

**Datasets** We use ImageNet-100, a 100-class subset of ImageNet [56, 60], to pretrain the standard ResNet-50 [34] architecture of self-supervised methods: MoCo-v2 [16], SimCLR [14], Barlow Twins [71], as well as for common in the literature on augmentation-aware self-supervised learning [60, 67, 41, 13]. For MoCo-v3 [18], we pretrain the ViT-Small [22] model on the full ImageNet dataset [56].

**Hyperparameters** We follow the pretraining procedures from corresponding papers, described in [41] for MoCo-v2, [13] for SimCLR, [71] for Barlow Twins, and [18] for MoCo-v3. Synchronized batch normalization is employed for distributed training [17]. In Table 5, we present the training hyperparameters which are not related specifically to CASSLE, but rather joint-embedding approaches in general [33, 16, 14, 71, 17, 18].

Table 5: Hyperparameters of self-supervised methods used with CASSLE

SSL method	Architecture	Number of epochs	Batch size	Weight decay	Learning rate		Training time
					Base	Schedule	
MoCo-v2 [16]	ResNet-50	500	256	$10^{-4}$	0.03	Cosine decay	34h
SimCLR [14]	ResNet-50	300	1024	$10^{-4}$	0.05	Cosine decay	10h
Barlow Twins [71]	ResNet-50	500	256	$10^{-4}$	0.05	Cosine decay with warmup	36h
MoCo-v3 [18]	ViT-small	300	1024	0.1	$1.5 \cdot 10^{-4}$	Cosine decay with warmup	23h

SSL method	Projector				Predictor			
	Depth	Hidden size	Out size	Final BatchNorm	Depth	Hidden size	Out size	Final BatchNorm
MoCo-v2	2	2048	128	No				No
SimCLR	2	2048	128	No				No
Barlow Twins	3	8192	8192	Yes, without affine transform				No
MoCo-v3	3	4096	256	Yes, without affine transform	2	4096	256	Yes, without affine transform

**Augmentations** For self-supervised pretraining, we use a set of augmentations adopted commonly in the literature [33, 14, 16, 17, 71, 41]. We denote them below:

- **random cropping** – We sample the cropping scale randomly from [0.2, 1.0]. Afterward, we resize the cropped images to the size of  $224 \times 224$ .
- **color jittering** – We apply this operation with a probability of 0.8. We sample the intensities of brightness, contrast, saturation, and hue and their maximal values are 0.4, 0.4, 0.4, and 0.1, respectively.
- **Gaussian blurring** – We apply this operation with a probability of 0.5. We sample the standard deviation from [0.1, 2.0] and set the kernel size to  $23 \times 23$ .
- **random horizontal flipping** – We apply this operation with a probability of 0.5.
- **random grayscaleing** – We apply this operation with a probability of 0.2.

### A.2 Evaluation

**Linear evaluation** The linear evaluation (linear probing) protocol used throughout this work follows [14, 30, 37, 41]. Namely, we center-crop and resize the images from the downstream dataset to the size of  $224 \times 224$ , pass them through the pretrained feature extractor, and obtain the embeddings from the final feature extractor stage. The only exception from this is the CUB dataset [64], where,

following [41], for the training images besides the center crop of the image, we also crop the image at its corners and do the same for the horizontal flip of the image (this is known as TenCrop operation<sup>6</sup>). Having gathered the image features, we minimize the  $l_2$ -regularized cross-entropy objective using L-BFGS on the features of the training images. We select the regularization parameter from between  $[10^{-6}, 10^5]$  using the validation features. Finally, we train the linear classifier on training and validation features with the selected  $l_2$  parameter and report the final performance metric (see Table 6) on the test dataset. We set the maximum number of iterations in L-BFGS as 5000 and use the model trained on training data as initialization for training the final model.

We note that the above linear evaluation procedure is effectively equivalent to training the final layer of a network on non-augmented data while keeping the remainder of the parameters unchanged.

We list the datasets and evaluation metrics used during linear evaluation in Table 6.

Table 6: Datasets and respective evaluation metrics used for linear evaluation of CASSLE.

Downstream task	Dataset	Evaluation metric
C10	CIFAR10 [39]	Top-1 accuracy
C100	CIFAR100 [39]	Top-1 accuracy
Food	Food101 [9]	Top-1 accuracy
MIT	MIT67 [52]	Top-1 accuracy
Pets	Oxford-IIIT Pets [50]	Mean per-class accuracy
Flowers	Oxford Flowers-102 [46]	Mean per-class accuracy
Caltech	Caltech101 [25]	Mean per-class accuracy
Cars	Stanford Cars [38]	Top-1 accuracy
FGVCA	FGVC-Aircraft [43]	Mean Per-class accuracy
DTD	Describable Textures (split 1) [19]	Top-1 accuracy
SUN	SUN397 (split 1) [66]	Top-1 accuracy
CUB	Caltech-UCSD Birds [64]	Top-1 accuracy
300W	300 Faces In-the-Wild [57]	$R^2$

**Object detection** We closely follow the evaluation protocol of [33]. We train the Faster-RCNN [54] model with the pretrained backbone. Contrary to [33], we do not tune the backbone parameters, in order to better observe the effect of different pretraining methods. We report the Average Precision [42] measured on the VOC test2007 set [24].

**Sensitivity to augmentations** We consider image pairs, where one image is the (center-cropped) original and the second one is augmented by the given augmentation. For each image pair, we extract image features at four stages of the pretrained ResNet-50 backbone [34], as well as the final representation of the projector network. We next calculate cosine similarities between the features of augmented and non-augmented images in the given mini-batch (of size 256). We report the value of the InfoNCE loss [62] calculated on such similarity matrices.

**Dependency of CASSLE projector on conditioning** Similarly to the above experiment, we compare the projector features of augmented and non-augmented image pairs. When computing the features of the augmented image, we supply the projector with the augmentation embedding computed from augmentation parameters corresponding to either this image (true augmentation information) or another, randomly chosen image from the same mini-batch (random augmentation information). We then compute cosine similarities between the original image features and features of the augmented image computed with true/random augmentation information.

### A.3 Implementation details

We implement CASSLE in the PyTorch framework [51], building upon the codebase of [41]. Our code is available at [github.com/gmum/CASSLE](https://github.com/gmum/CASSLE). We train variants of all SSL approaches on 2

<sup>6</sup><https://pytorch.org/vision/main/generated/torchvision.transforms.TenCrop.html>

NVidia A100 GPUs, except for SimCLR and MoCo-v3 which use larger batch sizes and therefore require 8 such GPUs.

## B Additional analysis of CASSLE

In this section, we highlight several additional features of CASSLE, including its effect on the pretraining loss minimization, generalization to unseen augmentations, and robustness to perturbed images. We also compare CASSLE with the masked image modeling family of SSL methods [59], and demonstrate its applicability to joint-embedding SSL approaches that do not utilize the projector in their architecture [33].

### B.1 Analysis of the self-supervised learning procedure

We compare the training of MoCo-v2 [33, 16] with and without CASSLE or AugSelf [41] extensions, and plot the contrastive loss values measured throughout training in the left part of Figure 7, and on the right, the values of losses relative to the vanilla MoCo-v2. CASSLE minimizes the contrastive objective faster than the other two variants, in particular early in the training procedure. This suggests that augmentation information provides helpful conditioning for a model not yet fully trained to align augmented image pairs and thus, CASSLE learns to depend on this information.

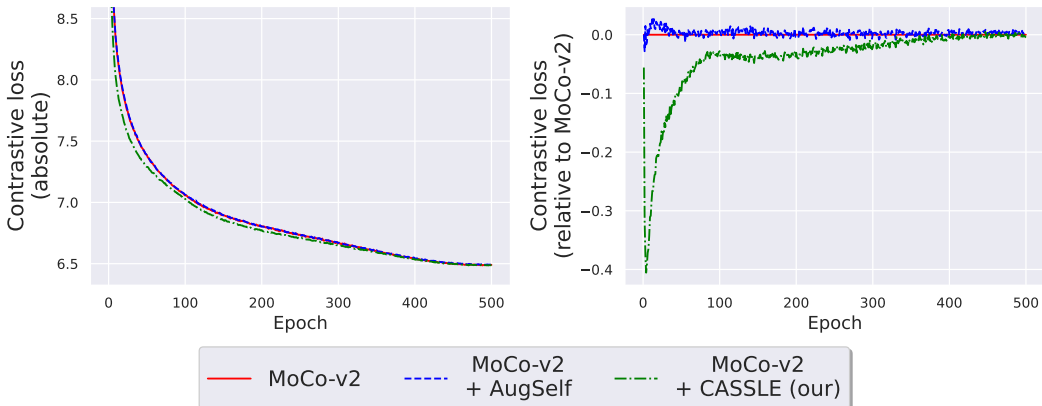


Figure 7: Absolute (left) and relative to Baseline (right) values of contrastive losses of Baseline, AugSelf [41], and CASSLE MoCo-v2 variants, measured during pretraining. CASSLE minimizes the contrastive objective faster than Baseline and AugSelf, in particular early in the training procedure.

### B.2 Modulating the augmentation-awareness

As seen in Section 4.2, CASSLE increases the augmentation-awareness of feature extractor representations. This raises a question – *can we influence the level of augmentation-awareness?*

In CASSLE, the task of augmentation-awareness is not enforced by any specific objective function. We consider this as an advantage of CASSLE – the model can learn to use the augmentation information to a degree that is useful for solving the invariance task. On the other hand, in AugSelf [41], there is a need to balance the invariance and sensitivity objectives with a hyperparameter. In CASSLE, we can modulate the emergent augmentation-awareness by modifying the expressiveness of the augmentation encoder network. Thus, if the amount of available augmentation information during training is reduced, the model should learn not to rely on it and become more augmentation-invariant. To verify this, we train several variants of MoCo-v2+CASSLE with increased and compressed Augmentation encoder output sizes. Next, similarly to the experiment described in Section 4.2, we compare the InfoNCE loss of matching the feature extractor output representations of augmented image pairs. We show the results for different augmentation types in Figure 8. Models trained with a less expressive Augmentation encoder are also more augmentation-invariant, as evidenced by lower InfoNCE values. This can be attributed to the fact that augmentation information compressed low-dimensional embedding may be less informative for solving the augmentation invariance task.

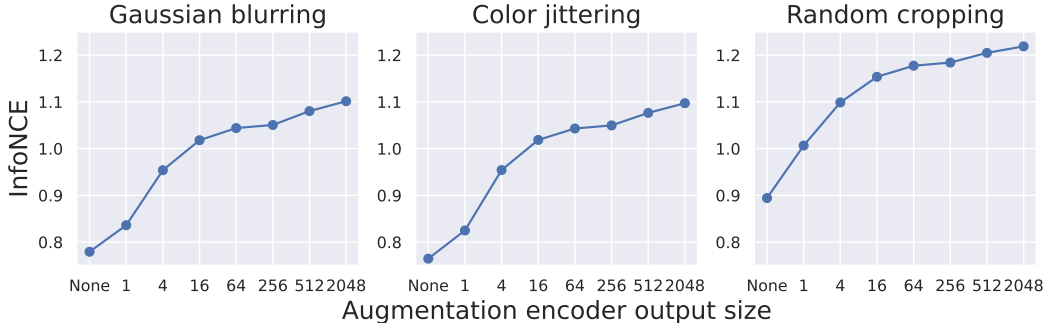


Figure 8: A comparison of InfoNCE loss measured on different kinds of augmentations at the output of the feature extractor. We compare variants of MoCo-v2+CASSLE with different Augmentation encoder output sizes, as well as the vanilla MoCo-v2 (denoted as *None*). CASSLE with increasing Augmentation encoder sizes yield higher InfoNCE values, which suggests that this hyperparameter influences the augmentation sensitivity of CASSLE.

### B.3 Generalization to unseen augmentations

Table 7: Linear evaluation on the task of predicting image rotation (0/90/180/270 degrees)

Method	C10	C100	Food	Pets	MIT	Flowers	Caltech	Cars	FGVCA	STL10	SUN
<i>SimCLR</i> [14]											
Vanilla	67.93	56.88	68.76	65.07	<b>70.40</b>	24.15	56.81	87.12	98.02	<b>73.90</b>	67.94
AugSelf [41]	75.63	63.08	75.01	57.99	16.54	<b>33.99</b>	39.03	76.11	96.64	67.88	76.60
<b>CASSLE</b>	<b>77.07</b>	<b>70.20</b>	<b>79.55</b>	<b>70.97</b>	68.77	33.08	<b>64.97</b>	<b>95.14</b>	<b>99.46</b>	72.69	<b>78.16</b>
<i>MoCo-v2</i> [33, 16]											
Vanilla	67.96	56.96	75.70	71.27	67.13	<b>58.30</b>	<b>87.33</b>	58.35	93.20	<b>95.44</b>	68.33
AugSelf [41]	<b>74.57</b>	65.87	73.03	<b>77.01</b>	<b>79.75</b>	52.81	58.53	<b>93.07</b>	98.26	77.35	<b>83.66</b>
<b>CASSLE</b>	73.21	<b>69.91</b>	<b>77.31</b>	76.04	76.40	45.11	61.06	90.49	<b>98.56</b>	63.65	76.01
<i>Barlow Twins</i> [71]											
Vanilla	73.67	64.87	72.85	<b>83.02</b>	70.97	42.56	<b>57.71</b>	83.68	97.93	65.70	76.87
AugSelf [41]	72.79	<b>65.91</b>	74.93	77.76	50.30	30.93	44.31	85.85	98.35	<b>69.68</b>	<b>77.19</b>
<b>CASSLE</b>	<b>74.97</b>	65.15	<b>76.55</b>	77.05	<b>86.49</b>	<b>43.16</b>	53.60	<b>92.92</b>	<b>99.16</b>	55.24	74.97

To understand whether CASSLE generalizes to types of augmentation that were not used during pretraining, we inspect its performance in the task of prediction of the applied augmentation. We train a linear classifier on top of the pretrained model to predict whether the image was rotated by 0, 90, 180, or 270 degrees. We formulate the problem as classification due to its cyclic nature and test the model on the same datasets as in Section 4.1. We present the results of vanilla, AugSelf [41] and CASSLE variants of self-supervised methods in Table 7. Apart from a few exceptions, CASSLE and AugSelf extensions allow in general for better rotation prediction than the vanilla SSL methods. Moreover, in the case of SimCLR and Barlow Twins, the CASSLE representation predicts the rotations the most accurately on a vast majority of datasets. This occurs despite the fact, that neither of the methods was trained using rotated images and thus, never explicitly learned the *concept* of rotation. This suggests that CASSLE learns representations that are sensitive to a broader set of perturbations than those whose information had been used during pretraining.

### B.4 Robustness under perturbations

We next verify the influence of increased sensitivity to augmentations on the robustness to perturbations of models pretrained with MoCo-v2 [33, 16] and SimCLR [14]. Following the experimental setup of [41], we train the pretrained networks for classification of ImageNet-100 and evaluate them on weather-corrupted images (fog, frost, snow, and brightness) [35] from the validation set. We report the results in Table 8. We find that the network pretrained with MoCo-v2+CASSLE achieves the

best results when dealing with images perturbed by brightness and snow, whereas vanilla MoCo-v2 performs best on images perturbed by fog and frost. When it comes to SimCLR, except for the images perturbed by frost, CASSLE achieves the best performance.

Table 8: Evaluation of variants of MoCo-v2 and SimCLR on perturbed ImageNet-100 images.

Method	MoCo-v2 [33, 16]				SimCLR [14]			
	Brightness	Frost	Fog	Snow	Brightness	Frost	Fog	Snow
Vanilla	85.30	<b>53.70</b>	<b>56.92</b>	31.78	85.74	<b>50.66</b>	53.94	33.78
AugSelf	83.64	51.98	53.08	33.80	85.84	50.34	53.60	32.98
CASSLE	<b>86.10</b>	50.54	54.22	<b>34.66</b>	<b>86.38</b>	48.62	<b>59.04</b>	<b>35.30</b>

### B.5 Comparison with Masked Image Modeling

Recently, Masked Image Modeling (MIM) methods have emerged as a new family of approaches to Self-supervised Learning [69, 32, 59]. Contrary to Joint-Embedding methods, MIM-based methods rely on missing data imputation as their pretext task. Thus, a natural question arises, whether MIM-based methods are not a better tool to address the cases where augmentation-invariance is expected to be problematic?

To answer this, we compare the vanilla MoCo-v2, and MoCo-v2+CASSLE with Sparse masked modeling (SparK) [59] – a recently introduced method for Masked Image Modeling for convolutional networks. For consistency, we use the ResNet-50 backbone with all models and pretrain SparK with hyperparameters suggested by the authors [59]. We compare the methods in terms of augmentation invariance and linear evaluation, analogously to Sections 4.2 and 4.1, respectively.

Given that SparK does not rely on the augmentation-invariance objective, we do not expect its representations to be invariant to augmentations.

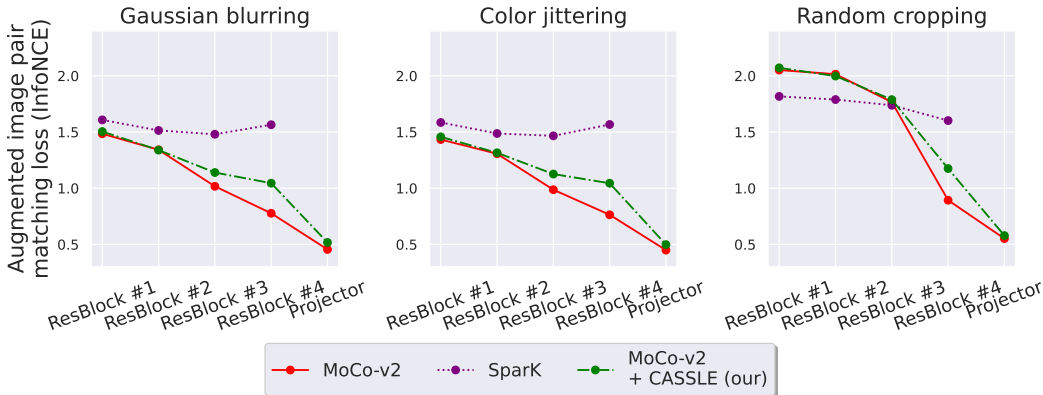


Figure 9: Comparison of augmentation-awareness of vanilla and CASSLE variants of MoCo-v2 [33, 16] and SparK [59]. Since SparK is not trained through a Joint-Embedding objective of augmentation-invariance, its representations exhibit higher sensitivity to changes in data caused by augmentations compared to the joint-embedding MoCo-v2.

We confirm this in Figure 9 – SparK yields high values of the InfoNCE loss of matching the embeddings of augmented image pairs. This indicates that its representations are highly sensitive to features transformed by augmentations.

However, the linear evaluation results shown in Table 9 show that SparK representations perform much worse in the majority of downstream tasks compared to both vanilla MoCo-v2 and MoCo-v2+CASSLE. Indeed, poor linear evaluation accuracy of MIM-based models compared to Joint-Embedding models is their known drawback [49, 59].

Joint-Embedding methods, even when extended with CASSLE, form more augmentation-invariant representations compared to MIM-based methods. Nevertheless, Joint-Embedding methods offer better transfer learning performance, which can be further boosted by extending them with CASSLE.

Table 9: Linear evaluation comparison of vanilla and CASSLE variants of MoCo-v2 [33, 16] and SparK [59]. All models utilize the ResNet-50 architecture [34]. Both versions of MoCo-v2 exhibit better results than SparK, with MoCo-v2+CASSLE performing best on the majority of downstream tasks.

Method	C10	C100	Food	MIT	Pets	Flowers	Caltech	Cars	FGVCA	DTD	SUN	CUB	300W
MoCo-v2 [33, 16]	84.60	61.60	59.67	61.64	70.08	82.43	77.25	33.86	41.21	64.47	46.50	32.20	88.77 <sup>†</sup>
<b>MoCo-v2+ CASSLE</b>	<b>86.32</b>	<b>65.29</b>	<b>61.93</b>	<b>63.86</b>	<b>72.86</b>	<b>86.51</b>	<b>79.63</b>	<b>38.82</b>	<b>42.03</b>	<b>66.54</b>	<b>49.25</b>	<b>36.22</b>	88.93
SparK [59]	84.39	60.52	49.20	52.84	51.55	74.28	74.89	23.72	33.69	57.82	39.12	23.09	<b>96.13</b>

## B.6 Augmentation-aware conditioning without the projector

Joining image and augmentation embeddings through point-wise addition or multiplication allows us to implement CASSLE in Joint-Embedding frameworks that do not utilize the projector in their architecture, such as MoCo-v1 [33]. We compare the vanilla, AugSelf, and CASSLE (point-wise addition) variants of MoCo-v1 in Table 10. Surprisingly, CASSLE lends a major performance boost to MoCo-v1 despite that it does not utilize a projector network. This suggests that the CASSLE augmentation encoder can directly modulate the image embeddings through simple addition. This is further evidenced by Figure 10, where CASSLE increases the sensitivity to augmentations of the final stage of network representation by a significant margin. On the other hand, augmentation embeddings produced by CASSLE lead to making representations more similar, as visible at the projector stage.

Table 10: Linear evaluation of MoCo-v1 [33] on downstream classification and regression tasks. CASSLE improves the performance of the model by a large margin.

Method	C10	C100	Food	MIT	Pets	Flowers	Caltech	Cars	FGVCA	DTD	SUN	CUB	300W
MoCo-v1 [33]	58.82	28.09	25.90	31.04	47.25	33.29	44.41	5.00	10.98	36.86	19.00	9.16	88.05
MoCo-v1 + AugSelf [41]	64.94	37.01	32.84	33.13	45.95	38.59	45.15	8.33	15.14	40.37	20.48	11.27	88.12
<b>MoCo-v1+CASSLE</b>	<b>80.53</b>	<b>53.55</b>	<b>52.11</b>	<b>51.94</b>	<b>57.58</b>	<b>60.56</b>	<b>60.33</b>	<b>18.68</b>	<b>28.68</b>	<b>53.94</b>	<b>36.71</b>	<b>18.88</b>	<b>88.21</b>

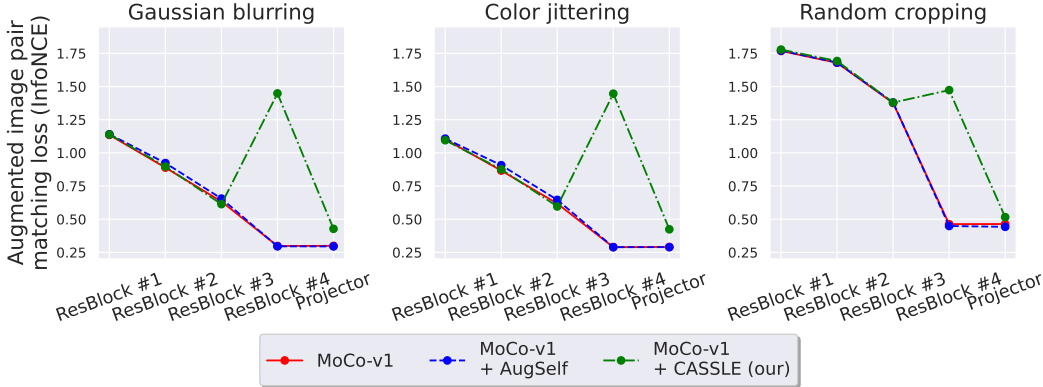


Figure 10: Comparison of augmentation-awareness of vanilla, AugSelf [41], and CASSLE variants of MoCo-v1, which does not contain a projector network. In the case of the vanilla and AugSelf variants, the representation of the fourth ResNet block stage is equivalent to the representation at the projector stage, whereas in CASSLE, the projector stage represents the fourth ResNet block stage with added augmentation embeddings.